THE JOURNAL OF BIOLOGICAL CHEMISTRY VOL. 286, NO. 50, pp. 43081–43090, December 16, 2011

Protein Interactions and Localization of the *Escherichia coli* Accessory Protein HypA during Nickel Insertion to [NiFe] Hydrogenase*[S]

Received for publication, August 5, 2011, and in revised form, October 12, 2011 Published, JBC Papers in Press, October 20, 2011, DOI 10.1074/jbc.M111.290726

Kim C. Chan Chung and Deborah B. Zamble[1]

From the Department of Chemistry, University of Toronto, Toronto, Ontario M5S 3H6, Canada

Background: HypA contributes to the biosynthesis of [NiFe] hydrogenase.
Results: *Escherichia coli* HypA interacts with the hydrogenase precursor protein, assembles other nickel insertion proteins, and localizes near the cell membrane.
Conclusion: HypA serves as a scaffold for nickel insertion, which occurs proximal to the cell membrane.
Significance: This information is crucial for understanding the biosynthesis of [NiFe] hydrogenase enzymes and nickel homeostasis in *E. coli*.

Nickel delivery during maturation of *Escherichia coli* [NiFe] hydrogenase 3 includes the accessory proteins HypA, HypB, and SlyD. Although the isolated proteins have been characterized, little is known about how they interact with each other and the hydrogenase 3 large subunit, HycE. In this study the complexes of HypA and HycE were investigated after modification with the *Strep*-tag II. Multiprotein complexes containing HypA, HypB, SlyD, and HycE were observed, consistent with the assembly of a single nickel insertion cluster. An interaction between HypA and HycE did not require the other nickel insertion proteins, but HypB was not found with the large subunit in the absence of HypA. The HypA-HycE complex was not detected in the absence of the HypC or HypD proteins, involved in the preceding iron insertion step, and this interaction is enhanced by nickel brought into the cell by the NikABCDE membrane transporter. Furthermore, without the hydrogenase 1, 2, and 3 large subunits, complexes between HypA, HypB, and SlyD were observed. These results support the hypothesis that HypA acts as a scaffold for assembly of the nickel insertion proteins with the hydrogenase precursor protein after delivery of the iron center. At different stages of the hydrogenase maturation process, HypA was observed at or near the cell membrane by using fluorescence confocal microscopy, as was HycE, suggesting membrane localization of the nickel insertion event.

Escherichia coli encodes at least three hydrogenase isoforms that are produced under anaerobic fermentative conditions (1, 2). All three hydrogenases are localized at the inner membrane of the cell, with the periplasmically oriented "uptake" hydrogenase 1 and 2 enzymes responsible for hydrogen oxidation to protons and electrons and the cytoplasmic hydrogenase 3 responsible for fermentative hydrogen production (1, 3). The large subunits of these heterodimeric enzymes harbor the dinuclear active site consisting of an $Fe(CN)_2(CO)$ cluster coordinated with a nickel ion (4, 5). The assembly of this [NiFe] metallocenter requires multiple accessory proteins (for reviews, see Refs. 6–8), and the HypA/HybF, HypB, and SlyD proteins are involved in nickel delivery to the precursor protein (6, 9). Nickel insertion is required before the hydrogenase enzyme large subunit can be processed by proteolytic cleavage to complete maturation (10). This biosynthetic pathway is thought to be reproduced in many organisms, which express homologues of HypA, HypB, and in some cases SlyD (6, 9). Although studies characterizing the individual nickel insertion proteins have emerged, there is limited information about how they act together to deliver nickel.

Deletion of any of the three nickel insertion genes results in strains of *E. coli* exhibiting decreased hydrogenase processing and activity that can be restored upon the addition of excess nickel to the growth medium (11–13). All three of these proteins can bind nickel *in vitro*, and all of the metal-binding sites, or in the case of SlyD the metal binding domain, are important for hydrogenase maturation (14–16). The participation of SlyD in hydrogenase biosynthesis was discovered through its interaction with HypB (13, 16). HypB and HypA can also interact (17, 18), suggesting a communal function for these two proteins and SlyD during nickel delivery to hydrogenase. Furthermore, multiprotein complexes including HycE and some combination(s) of HypA, HypB, and SlyD have been demonstrated (19). However, it was not clear if nickel insertion to the enzyme occurs via a cooperative multiprotein event.

In addition to nickel, HypA binds zinc with nanomolar affinity at a site composed of the cysteines from two conserved *CXXC* motifs (17, 20–22). This type of zinc binding motif is commonly found in domains that facilitate biomolecular interactions (23). In *E. coli*, HypA contributes to the biosynthesis of hydrogenase 3, whereas the homologous protein HybF fulfills the analogous role for production of hydrogenases 1 and 2 (12). The hydrogenase isoform specificity of HypA/HybF as well as the putative structural zinc site lead to the hypothesis that HypA and HybF interact directly with the appropriate

* This work was funded in part by grants from Canadian Institutes of Health Research and the Canada Research Chairs Program.
[S] The on-line version of this article (available at http://www.jbc.org) contains supplemental Table S1 and Figs. S1–S8.
[1] To whom correspondence should be addressed: 80 St. George St., Toronto, Ontario M5S 3H6, Canada. Tel.: 416-978-3568; E-mail: dzamble@chem.utoronto.ca.

TABLE 1
***E. coli* strains and plasmids used in this study**

Strain/plasmid	Genotype	Reference/source
***E. coli* strains**		
MC4100	F$^-$, *ara*D193, Δ(*argF*-lac)-*U169*, *pts*F25, *rel*A1, *flb*B5301, *rps*L150, λ$^-$	(55)
HD705	MC4100, Δ*hycE*	(56)
DHP-B	MC4100, Δ*hypB*	(57)
DPABF	MC4100, *hypA* (ATG → TAA), Δ*hybF*	(12, 57)
HYD723	MC4100, *nikA*::Mud*I*	(26)
DHP-C	MC4100, Δ*hypC*	(57)
Δ*hypD*	W3110 Δ*lacU169*, *gal*490, λ cI857, Δ(cro-bioA), Δ*hypD*, *hypE-SPA*	(46)
Δ*slyD*	W3110 Δ*lacU169*, *gal*490, λ cI857, Δ(cro-bioA) , Δ*slyD*	(13)
Δ*hyaB* Δ*hybC* Δ*hycE*	Δ*hybClacI*^{q}, $rrnB_{T14}$, Δ$lacZ_{W116}$, *hsdR514*, Δ$araBAD_{A1133}$, Δ$rhaBAD_{LD78}$, *hyaB hybC hycE* Δ*kan*	(58)
Plasmids		
pBAD24	Amp^R, *araC*	(24)
pBAD24-HycEStr	Amp^R, *araC*, pBAD24, *Strep*-tag *II hycE*	(19)
pBAD24-HypBStr	Amp^R, *araC*, pBAD24, *Strep*-tag *II hypB*	(19)
pET24b-*hypA*	Kan^R, pET24b, *hypA*	This work
pBAD18	Kan^R, *araC*	(24)
pBAD18-HypA	Kan^R, *araC*, pBAD18, *hypA*	This work
pBAD18- HypAStr	Kan^R, *araC*, pBAD18, *Strep*-tag *II hypA*	This work
pBAD18- HypA H2A	Kan^R, *araC*, pBAD18, *hypAH2A*	This work

hydrogenase large subunit (12, 14), but this model has not been tested.

In this study we provide evidence for an interaction between HypA and HycE and demonstrate that this interaction occurs in the presence of, but does not require, the other known nickel insertion proteins. The HypA-HycE complex is only observed in cells competent for iron insertion to the premature enzyme, and it is influenced by the NikABCDE transporter. Furthermore, pulldown assays performed with a tagged variant of HypA result in the co-elution of multiple proteins associated with the inner membrane, suggesting localization of HypA at or near this cellular milieu. This model was confirmed by fluorescence microscopy of *E. coli*, which revealed that HypA as well as HycE are at the membrane during different stages of hydrogenase maturation. The implications of these data on the role for HypA during nickel insertion to the hydrogenase precursor protein are discussed.

EXPERIMENTAL PROCEDURES

Materials—Primers were purchased from Sigma. *Pfu* DNA polymerase was from Fermentas, and restriction enzymes were from New England Biolabs. *Strep*-tactin-Sepharose columns and *Strep*MAB antibodies were purchased from IBA. Anti-HypB rabbit polyclonal antibodies (11) were a generous gift from Prof. A. Böck (University of Munich). Anti-SlyD rabbit polyclonal antibodies were prepared by immunization of rabbits with purified SlyD (Division of Comparative Medicine, University of Toronto) (16). Monoclonal anti-SlyD antibodies were generous gifts from Prof. M. Wahlgren (Karolinska Institutet). Anti-HypA and anti-HycE antibodies were prepared by immunizing rabbits with synthesized peptides (^{102}ADDGLQIRRIEIDQE^{116} from the HypA sequence or ^{395}RASGHARDTRADHPFVGY^{412} from the HycE sequence) (Cedarlane, Burlington ON). These sequences were chosen based on their lack of similarity with other proteins, as verified with BLAST, and their hydrophilicity. All fluorescent cell stains were purchased from Invitrogen. Solutions were prepared with Milli-Q water, 18.2 megohms·cm resistance (Millipore), and the pH values of the buffers were adjusted with HCl or NaOH.

Bacterial Strains and Plasmids—For a complete list of bacterial strains used in this study, see Table 1. Construction of the pBAD24-*Strep*-tag II *hycE* (pBAD24-*hycEStr*) plasmid was previously reported (19) and encodes a protein tagged with the 1172-Da *Strep*-tag II at the N terminus. The *hypAStr* gene was amplified by PCR from MC4100 with the forward 5′-GGGCGGCCATATGCACGAAATAACCCTCTGCCAACGGG-3′ and reverse 5′-CATCATCTCGAGTTACTTTTCGAACTGCGGGTGGCTCCACTCCTGGTCTATTTC-3′ primers. The PCR product was purified by using the QIAquick PCR purification kit (Qiagen) and digested with NdeI and XhoI. After subsequent purification, the fragments were ligated with pET24b (Novagen) digested with the same enzymes and transformed into XL-2 Blue *E. coli* (Stratagene). To subclone into the pBAD18-Kan plasmid (24), *hypA* (pBAD18-*hypA*) or *Strep*-tag II *hypA* (pBAD18-*hypAStr*, encoding the C-terminal-tagged HypA) was amplified by PCR from pET24b-*hypAStr* with the forward 5′-CGTATAGGCTAGCAGGAGGAATTCACCATGCACGAAATAACCCTCTG-3′ and either 5′-CGGCTCGTCTAGATCACTCCTGGTCTATTTCTATCCGC-3′ (*hypA*) or 5′-CAGCGCGTCTAGATTACTTTTCGAACTGCGGGTGGCTC-3′ (*Strep*-tag II *hypA*) reverse primers. The PCR products were purified and digested with NheI and XbaI. After subsequent purification, the fragments were ligated with pBAD18-Kan digested with the same enzymes and transformed into XL-2 Blue *E. coli*. Plasmid DNA was isolated from cultures grown in kanamycin-supplemented LB medium by using a Qiagen Plasmid Miniprep kit, and the sequences were verified (ACGT, Toronto, Canada). To introduce the H2A mutation into the pBAD18-*hypA* plasmid, QuikChange mutagenesis was performed using the forward (5′-CAGGAGGAATTCACCATGGCCGAAATAACCCTCTGCC-3′) and reverse (5′-GGCAGAGGGTTATTTCGGCCATGGTGAATTCCTCCTG-3′) primers.

Media, Growth Conditions, and Cross-linking—Cells were grown anaerobically at 37 °C for 16 h after inoculation with 1% (v/v) of an 8-h culture in sealed 1-liter bottles of buffered medium containing 10 g of Tryptone, 5 g of yeast extract, 69 mM

K_2HPO_4, and 22 mM KH_2PO_4/liter (13) supplemented with 1 μM sodium molybdate, 1 μM sodium selenite, 30 mM sodium formate, 0.8% glycerol, 100 μM arabinose, and either 100 μg/ml ampicillin (pBAD24-*hycEStr*) or 50 μg/ml kanamycin (pBAD18-*hypAStr*). The A_{600} of cell cultures under anaerobic growth did not surpass 1 absorbance unit. The cells were harvested by centrifugation, washed with 50 mM potassium phosphate, pH 7.6 (buffer A), and resuspended in buffer A containing 0.2 mM phenylmethylsulfonyl fluoride and trace amounts of DNase. For samples treated with cross-linker, 5 mM 1,5-difluoro-2,4-dinitrobenzene (Pierce) was added, and the cells were incubated at room temperature for 30 min followed by quenching with 100 mM Tris-HCl, pH 7.5. The cells were sonicated on ice or immediately stored at −80 °C for later use.

Hydrogenase Activity Assays—Total hydrogenase activity of crude cell extracts (not cross-linked) was monitored by measuring hydrogen-dependent reduction of benzyl viologen (2). Reactions were prepared in a septum-sealed cuvette in an anaerobic glove box (~96% N_2 and 4% H_2). Activity was measured in units/mg of total protein. One unit of activity corresponds to 1 μmol of benzyl viologen reduced/min, and an extinction coefficient of 7400 M^{-1} cm^{-1} was used (2). Protein concentrations were determined by the BCA protein assay (Pierce).

Purification of Strep-tag II Protein—After sonication of the cells and centrifugation for 30 min at 21,100 × *g* at 4 °C, the supernatant was applied to a *Strep*-tactin Superflow column (1 ml bed volume, IBA) aerobically. The column was washed with 25 column volumes of buffer A followed by 1 column volume each of 100 mM, 500 mM, and 1 M NaCl in buffer A and a final 2 column volumes of buffer A. In the case of samples prepared for native gel electrophoresis, the column was washed only with 5 column volumes of buffer A to maintain gentle purification conditions. The proteins were eluted with 3 column volumes of buffer A containing 2.5 mM desthiobiotin, and 0.5-ml fractions were collected. Tagged proteins eluted in fractions 3 and 4.

Western Analysis—Proteins were resolved on 10% or 12.5% SDS-polyacrylamide gels or 7.5% nondenaturing polyacrylamide gels and transferred to polyvinylidene difluoride membranes (Millipore) post-electrophoresis. The blots were probed with the appropriate polyclonal antibody at a 1:1000 dilution or 0.2 μg/ml monoclonal anti-*Strep*-tag II antibodies (IBA). HycEStr elution fractions were consistently analyzed by using the anti-*Strep*-tag II monoclonal antibody, but control experiments demonstrated that the same pattern of bands was observed as when the anti-HycE polyclonal antibodies were used. The 2° goat anti-rabbit or goat anti-mouse (Bio-Rad) antibodies were used at a dilution of 1:30,000. Enhanced chemiluminescence (Pierce) was used for detection.

In-gel Tryptic Digests—Proteins were resolved on 10% or 12.5% SDS-polyacrylamide gels, stained with Coomassie® Brilliant Blue R (Sigma) and destained with 25% ethanol. Gel pieces were washed in 50 mM ammonium bicarbonate and destained in 50% acetonitrile and 25 mM ammonium bicarbonate, transferred to a solution of 10 mM DTT in water for 30 min at 56 °C, incubated in 100 mM iodoacetamide in water for 15 min, and then incubated overnight at 37 °C with 0.2 μg/μl trypsin gold (Promega) in 50 mM ammonium bicarbonate. Digested peptides in solution were separated, and gel pieces were washed with alternating 5% formic acid and 100% acetonitrile to completely recover peptides. Samples were dried and reconstituted in 20 μl of 0.1% formic acid or stored dry at −20 °C until analysis.

LC-MS/MS—Confirmation of protein identity was carried out with tryptic peptides generated from an elution fraction from the *Strep*-tactin column digested with 10 ng/μl trypsin gold or in-gel tryptic digests and analyzed by LC-MS/MS. Samples were treated with Cleanup C18 Pipette Tips (Agilent), and 15 μl was injected onto an HPLC system (HP-Agilent 1100 series LC) interfaced by electrospray to a QTRAP LC-MS/MS system (LTQ Finnigan, Thermo Electron Corp.). A microbore (2.1-mm inner diameter × 50 mm) Thermo Gold C18 (2.2 μm) column with isocratic elution through a mobile phase of methanol/water (80:20, v/v) was used for LC separation. The samples were analyzed in the positive ion mode, and spectra were acquired in MS mode at 33 ms/scan and in MS/MS mode at 200 ms/scan. The data were processed to generate a peak list and fed into the SEQUEST search engine. The data were searched against the RCSB Protein Data Bank sequence data base.

Cell Staining and Preparation for Fluorescence Microscopy—Volumes of 57 ml were used for cultures grown anaerobically as outlined above. After harvesting, cells were washed twice in 15 ml of ice-cold PBS buffer (137 mM NaCl, 10 mM Na_2HPO_4, 2.7 mM KCl, 1.76 mM KH_2PO_4, pH 7.4). All of the following steps were performed with 1-ml volumes in PBS buffer at room temperature, and the cells were washed twice in between each step by resuspension, centrifugation at 10,770 × *g*, and decanting of supernatant. First, cells (1 ml of 10^{-1} dilution in PBS) were fixed in 4% formaldehyde for 10 min followed by permeabilization with 0.25% Triton X-100. Cells were then stained with 12.5 μM 4,4-difluoro-5-(2-thienyl)-4-bora-3a,4a-diaza-s-indacene-3-dodecanoic acid (BODIPY® 558/568 C_{12}) (Invitrogen) for 30 min followed by a second permeabilization step with 0.25% Triton X-100 and a final staining step with 2 μg/ml Alexa Fluor® 633 streptavidin conjugate for 30 min (Invitrogen). For immunofluorescence staining, after the second permeabilization step, 1 μg/ml primary monoclonal anti-SlyD antibody was incubated with cells for 1 h followed by final staining with 5 μg/ml Alexa Fluor® 633-labeled goat anti-mouse IgG (Invitrogen) for 45 min. Cells were applied to glass slides with 1:1 v/v of 0.3% agarose, and cover slides were sealed with nail polish. Cells were visualized with an Olympus IX81 inverted microscope using a 60× oil objective and illuminated with 543 nm and 633 nm helium neon laser sources (Advanced Optical Microscopy Facility, Toronto).

RESULTS

Hydrogenase 3 Large Subunit and HypA Form Multiprotein Complexes in the Cell—Previously, in an effort to capture and identify the nickel insertion proteins associated with the hydrogenase precursor protein, an N-terminal *Strep*-tag II variant of the hydrogenase 3 large subunit (HycEStr) with a molecular weight of 66 kDa in the unprocessed form was introduced into a bacterial strain with a genetic deletion of *hycE* (HD705). Pull-down studies with a *Strep*-tactin column revealed a mixture of processed and unprocessed HycEStr and a SlyD-HycE interac-

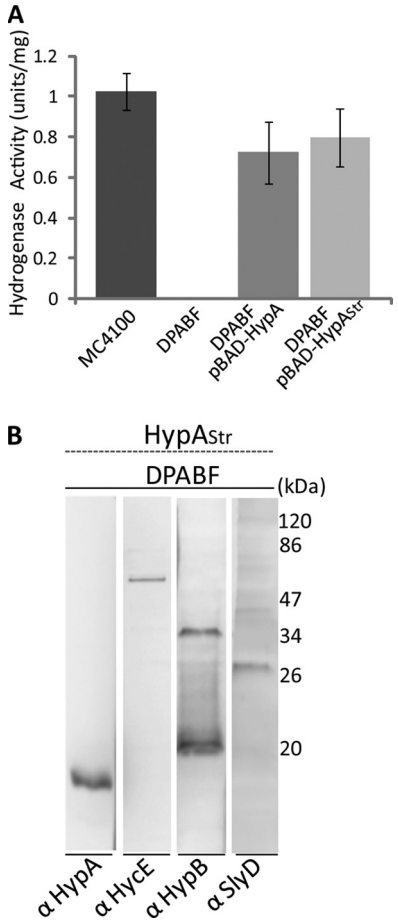

FIGURE 1. **HypAStr activity and protein complex formation.** *A*, crude cell lysates from wild-type MC4100 cells or DPABF (*hypA* ATG →TAA, Δ*hybF*) cells grown with or without the pBAD plasmid containing the *hypA or hypAStr* gene were prepared and tested for hydrogenase activity using benzyl viologen as the electron acceptor in an anaerobic solution assay containing 4% hydrogen gas. The results represent the average of three independent experiments, and *error bars* indicate ± 1 S.D. *B*, shown is a Western blot of the pulldown of HypAStr from DPABF using a *Strep*-tactin-Sepharose column. The expected molecular masses of the hydrogenase proteins are: HypAStr (14.3 kDa), HypB (31.6 kDa), SlyD (20.8 kDa), and hydrogenase isoform 3 large subunit HycE (65 kDa). The HypB protein is sensitive to proteolytic degradation, resulting in an additional 21-kDa fragment. SlyD typically migrates slower than expected on SDS-PAGE. Samples were reduced with β-mercaptoethanol and boiled before resolution on a 12.5% SDS-polyacrylamide gel followed by Western blotting with the indicated polyclonal antibodies.

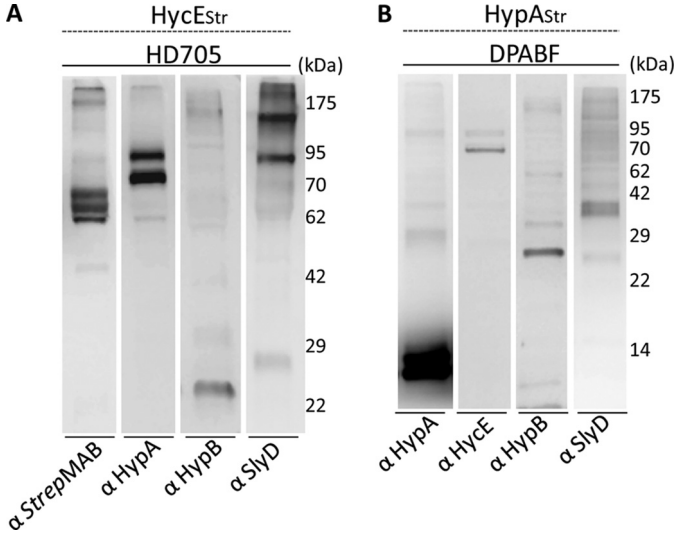

FIGURE 2. **HycEStr or HypAStr protein complexes.** Cells were exposed to a cell permeable cross-linker before lysis, and pulldown assays were performed by using a *Strep*-tactin-Sepharose column. Samples were reduced with β-mercaptoethanol and boiled before resolution on 10% (HycEStr pulldown assays) or 12.5% (HypAStr pulldown assays) SDS-polyacrylamide gels followed by Western blotting with the indicated antibodies. *A*, HD705 producing HycEStr is shown. *B*, DPABF producing HypAStr is shown.

tion occurring in early stages of hydrogenase maturation (19). HycEStr as bait also pulled out HypB and HypA along with SlyD, but it was unclear if all four proteins exist in a single complex or if they interact separately with HycE. The goals of this work were to resolve this issue and then to focus on the components and conditions required for the interaction between HypA and HycE.

A sequence coding for *Strep*-tag II was added onto the 3′ end of *hypA* and cloned into the arabinose-inducible pBAD18-Kan plasmid. Hydrogenase activity in DPABF (*hypA* ATG→TAA, Δ*hybF*) cells producing this C-terminal tagged HypA (HypAStr) is comparable with that from cells producing untagged HypA (Fig. 1*A*), demonstrating that HypAStr is functional in hydrogenase maturation. Pulldown experiments performed with lysate from DPABF cells producing HypAStr followed by Western blotting revealed co-elution of HypB, SlyD, and HycE (Fig. 1*B*). HycE co-eluted with HypAStr in the unprocessed form (supplemental Fig. S1). As a control, cell extracts from DPABF producing wild-type HypA and subjected to the same *Strep*-tactin column and Western blot analysis with anti-HypA, anti-HycE, anti-HypB, and anti-SlyD antibodies did not produce any detectable signal (data not shown). The observation that HypA, HypB, SlyD, and HycE can all be pulled down when either HypA (Fig. 1*B*) or HycE (19) are tagged suggests that there is complex formation between the nickel insertion proteins and the hydrogenase large subunit.

In an effort to trap these protein complexes, the membrane-permeable cross-linker 1,5-difluoro-2,4-dinitrobenzene was applied to cells. The use of cross-linker resulted in detection of increased amounts of co-eluting nickel insertion proteins with HycEStr (supplemental Fig. S2) after strenuous high salt wash conditions on the *Strep*-tactin column. After affinity chromatography, Western blots of cross-linked samples of HycEStr from HD705 cells transformed with pBAD24-*hycEStr* revealed the presence of multiprotein complexes containing HypA, HypB, and SlyD with HycEStr (Fig. 2*A*) and Chan Chung and Zamble (19). When HypAStr was cross-linked and pulled out of DPABF cells containing the pBAD18-*hypAStr* plasmid, all four proteins were again detected by Western blot (Fig. 2*B*) and confirmed by LC-MS/MS (supplemental Table S1). Occasionally, monomeric HypAStr was observed as a doublet in the Western blots, even in non-cross-linked samples (data not shown), which could be attributed to partial degradation during the purification process. It was not possible to identify a common band corresponding to a single multiprotein complex containing all of the HycE, HypA, HypB, and SlyD proteins in the denaturing Westerns, which suggests incomplete cross-linking of proteins, differences in antibody sensitivity in the Western blots, and/or the presence of other additional proteins in the complexes (19). As such, the Western assays with SDS-poly-

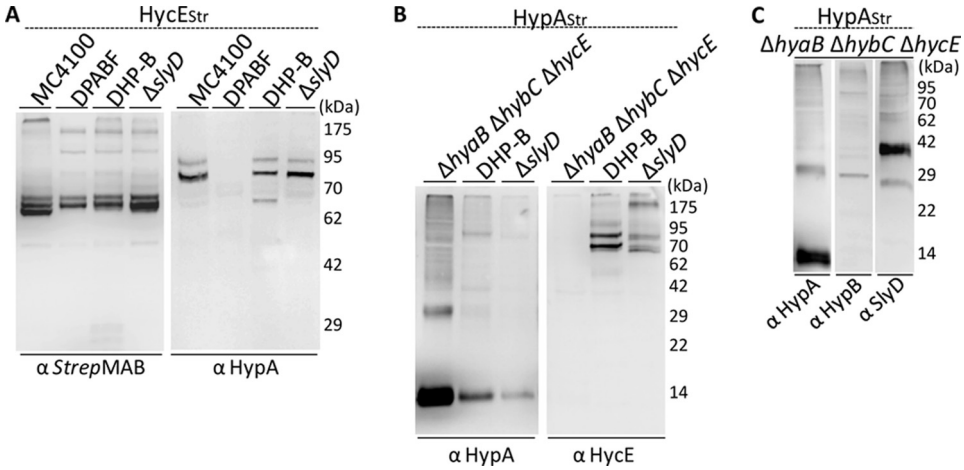

FIGURE 3. **HypA protein complexes formed in the absence of HypB, SlyD, or hydrogenase 1–3 large subunits.** Cells were exposed to a cell permeable cross-linker before lysis, and pulldown assays were performed by using a *Strep*-tactin-Sepharose column. Samples were reduced with β-mercaptoethanol and boiled before resolution on 10% (HycEStr pulldown assays) or 12.5% (HypAStr pulldown assays) SDS-polyacrylamide gels followed by Western blotting with the indicated antibodies. *A*, MC4100, DPABF, DHP-B, and Δ*slyD* strains producing HycEStr are shown. B, Δ*hyaB* Δ*hybC* Δ*hycE*, DHP-B, and Δ*slyD* strains producing HypAStr are shown. *C*, Δ*hyaB* Δ*hybC* Δ*hycE* expressing HypAStr is shown.

acrylamide gels were used as a means to assess the presence of specific proteins in the elution fractions. Samples of pulldown assays from cross-linked cells producing either HypAStr or HycEStr were also analyzed by native gel electrophoresis and Western blotting (supplemental Fig. S3). For either bait protein, although some smearing and multiple bands are observed, there is one band common to the Westerns probed with the antibodies to all four proteins, providing support for a single multiprotein complex.

HypA Forms Complexes with HycE without HypB or SlyD—To investigate whether HypA interacts with HycE in the absence of the other nickel insertion proteins, *in vivo* cross-linking and pulldown assays with HycEStr or HypAStr were performed in DHP-B (Δ*hypB*) and Δ*slyD* strains containing either pBAD24-*hycEStr* or pBAD18-*hypAStr*. To control for possible competition for HypA between plasmid-encoded HycEStr and genomically encoded HycE in DHP-B and Δ*slyD* strains, the wild-type MC4100 strain was transformed with pBAD-*hycEStr*. No significant difference was detected in the amount of HypA co-eluting from MC4100 or HD705 strains expressing HycEStr (Fig. 2*A* *versus* 3*A* anti-HypA Western blots). Furthermore, the interaction between HypA and HycE was maintained in both DHP-B and Δ*slyD* strains (Fig. 3, *A* and *B*). LC-MS/MS was used to confirm the association between HycE and HypA in the DHP-B or Δ*slyD* backgrounds (supplemental Table S1), indicating that the hydrogenase large subunit associates with HypA independent of the other nickel proteins and their activities. In contrast, when HycEStr pulldown experiments were performed from the DPABF strain, HypB could not be detected by Western blot (data not shown) or by LC-MS/MS (supplemental Table S1), supporting a role for HypA in mediating complex formation between HypB and HycE.

Nickel Insertion Protein Complexes Can Form in the Absence of Hydrogenase—To investigate if the nickel insertion proteins could assemble in the absence of hydrogenase, a bacterial strain containing gene deletions of three hydrogenase isoform large subunits (Δ*hyaB* Δ*hybC* Δ*hycE*) was transformed with pBAD18-*hypAStr* (Fig. 3*C*). After exposure to the cross-linker and pulldown of the tagged HypAStr as bait, Western blots revealed co-elution with HypB and SlyD (Fig. 3*C* and supplemental Table S1). This result indicates that HypA can form complexes with the other nickel insertion proteins HypB and SlyD in the absence of hydrogenase.

The Interaction between HypA and HycE Occurs after Iron Insertion—The current model for [NiFe] hydrogenase maturation presents the biosynthesis of the active site as two distinct events; the first is iron insertion enabled by the HypCDEF proteins, and the second is nickel insertion (25). To test this model and to verify that HypA participates during nickel insertion in the second stage of hydrogenase maturation, HycEStr was pulled down from DHP-C (Δ*hypC*) or Δ*hypD* cells containing pBAD24-*hycEStr*, representing a putative HycE precursor devoid of iron and unprepared for nickel insertion. Although constant amounts of total protein were loaded per lane, decreased relative amounts of HycEStr in both DHP-C and Δ*hypD* are evident (Fig. 4 and supplemental Fig. S4), possibly due to degradation of immature HycE or an increase in additional proteins, such as folding chaperones associated with the premature large subunit (19). Nevertheless, HypA was not detected at all in association with HycE from either of these strains by Western blotting or in the case of DHP-C by LC-MS/MS (Fig. 4, supplemental Fig. S4 and Table S1). Similarly, in the converse experiment, HypAStr was pulled down from a DHP-C strain, and co-eluting HycE was not detected (supplemental Fig. S5). It should be noted that HycE expression levels in the DHP-C strain are less than half that of the wild-type MC4100 (data not shown). Furthermore, as described above for HycEStr, decreased relative amounts of HypAStr were observed in the pulldown sample from the DHP-C strain compared with the MC4100 sample. To control for this difference, more total protein from the DHP-C pulldown sample compared with the wild-type samples was used for Western analysis, and HycE was still not observed (supplemental Fig. S5). Altogether, these observations are consistent with a role for HypA in the hydrogenase maturation process that is dependent on the participation of HypC and HypD. Similarly,

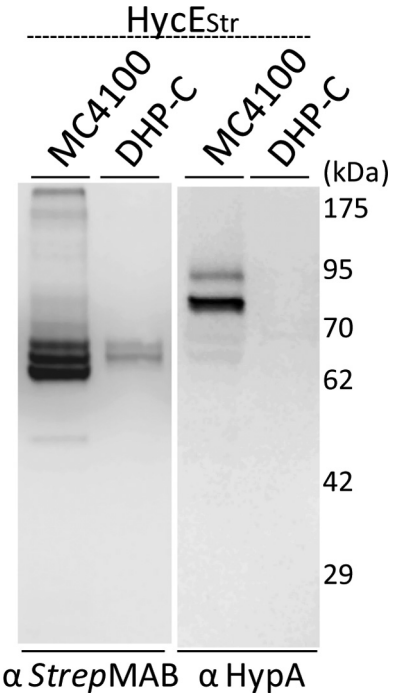

FIGURE 4. **The interaction between HypA and HycE occurs after iron insertion.** Wild-type MC4100 cells or DHP-C (Δ*hypC*) cells producing HycEStr were exposed to a cell permeable cross-linker before lysis, and pulldown assays were performed by using a *Strep*-tactin-Sepharose column. Samples were reduced with β-mercaptoethanol and boiled before resolution on 10% SDS-polyacrylamide gels followed by Western blotting with the indicated antibodies.

HypB was not detected by Western blot (data not shown) or by LC-MS/MS.

An Active NikABCDE Transporter Enhances the HypA-HycE Complex—To assess whether nickel imported by the NikABCDE transporter is required for the HypA interaction with HycE, a pulldown assay was performed with HycEStr expressed in the bacterial strain HYD723 (Δ*nikA*), which lacks the soluble periplasmic component of the transporter. Disruption of nickel uptake resulted in a loss of hydrogenase activity (Fig. 5*A*) as expected (26) as well as decreased processing of the enzyme large subunit (Fig. 5*B*), an event that follows nickel insertion (27). A marked decrease in the amount of HypA pulled down with HycEStr was observed in HYD723 compared with the MC4100 wild-type strain (Fig. 5*C*). Similarly, when HYD723 cells expressing HypAStr were treated with cross-linker and pulldown assays were performed, less co-eluting HycE was observed relative to a HypAStr pulldown from MC4100 (supplemental Fig. S6). This effect on the amount of detectable HypA-HycE complex supports a connection between the nickel imported by the Nik transporter and the interactions between the nickel insertion proteins and the hydrogenase large subunit. In contrast, the amount of HypB and SlyD pulled down with HypAStr from HYD723 cell lysates was not dramatically affected (supplemental Fig. S6), suggesting that nickel is not required for assembly of these proteins before association with the hydrogenase precursor.

To test whether exogenously added nickel could restore the HypA-HycEStr interaction, extra nickel was added to the growth media of the HYD723 cells. It is possible that high concentrations of nickel can leak through the Nik transporter even in the absence of the NikA periplasmic protein or alternatively through the high capacity Mg^{2+} transport system (28). In agreement with this hypothesis, nickel uptake is indicated by the restored hydrogenase activity (Fig. 5*A*) and HycEStr processing (Fig. 5*B*). However, only a very slight increase in the amount of HypA pulled down with HycE from the HYD723 strain grown with added nickel was observed (Fig. 5*C*). It should be noted that HycEStr production levels were lower in the HYD723 strains (Fig. 5*B*), which would also contribute to less detectable HypA. To verify that the decrease in co-eluting HypA was not solely due to lower HycEStr production levels, band intensities were compared using densitometry software. The difference between the HypA signals was more than 2-fold greater when comparing the MC4100 and HYD723 samples than the difference between HycEStr signals with or without nickel supplementation. The low amount of HypA-HycEStr complexes coupled with the hydrogenase processing and activity suggest that upon growth in higher concentrations of nickel some of the metal can bypass the nickel insertion proteins to reach the hydrogenase enzyme through unidentified means.

To investigate if nickel binding to HypA mediates the HypA-HycEStr interaction, the nickel-binding His-2 (14, 18) in HypA was mutated to an alanine (H2A), and the mutant protein was co-produced with HycEStr in the DPABF strain. The interaction between HycEStr and H2A-HypA was still observed (supplemental Fig. S7), which suggests that the association does not require metal binding by HypA.

HypAStr Pulls Down Membrane-associated Proteins—HypAStr pulldown experiments from DPABF cells not treated with cross-linker were resolved on SDS-polyacrylamide gels, and many protein bands were detected upon staining with Coomassie Blue dye (Fig. 6*A*). More protein bands relative to the bait protein in HypAStr pulldown assays were observed compared with HypBStr or HycEStr pulldown assays (Fig. 6). To identify some of these co-eluting proteins, bands were cut from the gels, and in-gel tryptic digests were performed followed by LC-MS/MS. Due to the abundance of proteins in the HypAStr elution fractions, clear HypB, SlyD, and HycE bands were not observed; however, as described above, tryptic digests of elution fractions followed by LC-MS/MS as well as Western blotting did confirm their presence (Ref. 19, Fig. 1, and supplemental Table S1). The HypAStr co-eluting proteins include membrane-associated proteins linked to the pyruvate formate lyase and formate hydrogen lyase pathways (see Fig. 6*A* and supplemental Table S1). Examples include aldehyde-alcohol dehydrogenase (a pyruvate formate-lyase deactivase) and formate dehydrogenase-H (a component (along with HycE) of the formate hydrogen lyase complex) (1, 29–31). Other membrane proteins, such as D-tagatose-1,6-bisphosphate aldolase subunit (involved in galactitol catabolism) and glycerol-3-phosphate dehydrogenase, were also identified (Fig. 6, *A* and *C*, and supplemental Table S1). These proteins are likely present because of cell growth on glycerol as a carbon source and metabolite (32–34).

HypA and HycE Are Localized at the Cell Membrane—The co-elution of membrane proteins with HypAStr prompted further investigation into the subcellular localization of HypA and

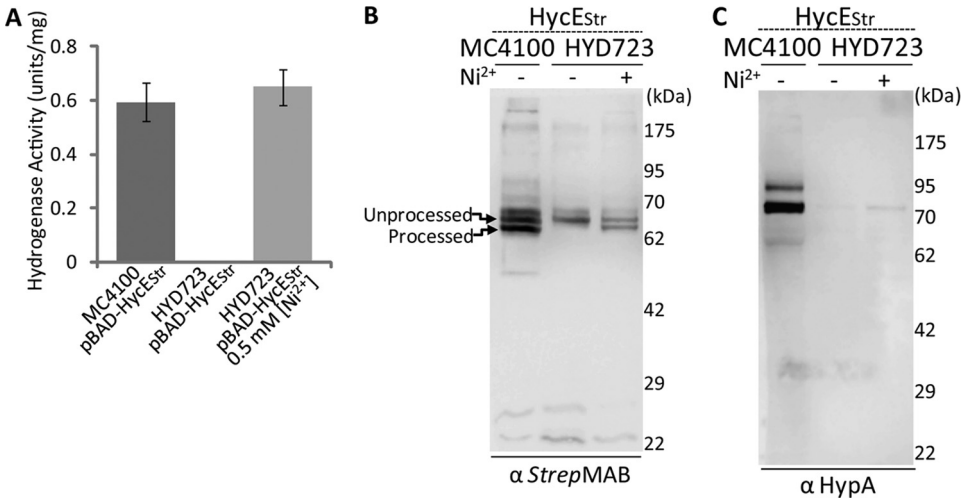

FIGURE 5. **An intact NikABCDE transporter enhances the formation of a HypA-HycE complex.** HycEStr was produced in MC4100 cells or HYD723 with or without supplementation of the growth media with 0.5 mM nickel. *A*, cell extracts were prepared and tested for hydrogenase activity using benzyl viologen as the electron acceptor in an anaerobic solution assay containing 4% hydrogen gas. The results represent the average of three independent experiments, and *error bars* indicate ± 1 S.D. Shown is an anti-*Strep*MAB Western blot with processed and unprocessed HycEStr (*B*) and anti-HypA Western (*C*) blot. For *B* and *C*, cells were exposed to a cell permeable cross-linker before lysis, and pulldown assays were performed by using a *Strep*-tactin-Sepharose column. Samples were reduced with β-mercaptoethanol and boiled 10% SDS-polyacrylamide gels before resolution on 10%SDS-polyacrylamide gel.

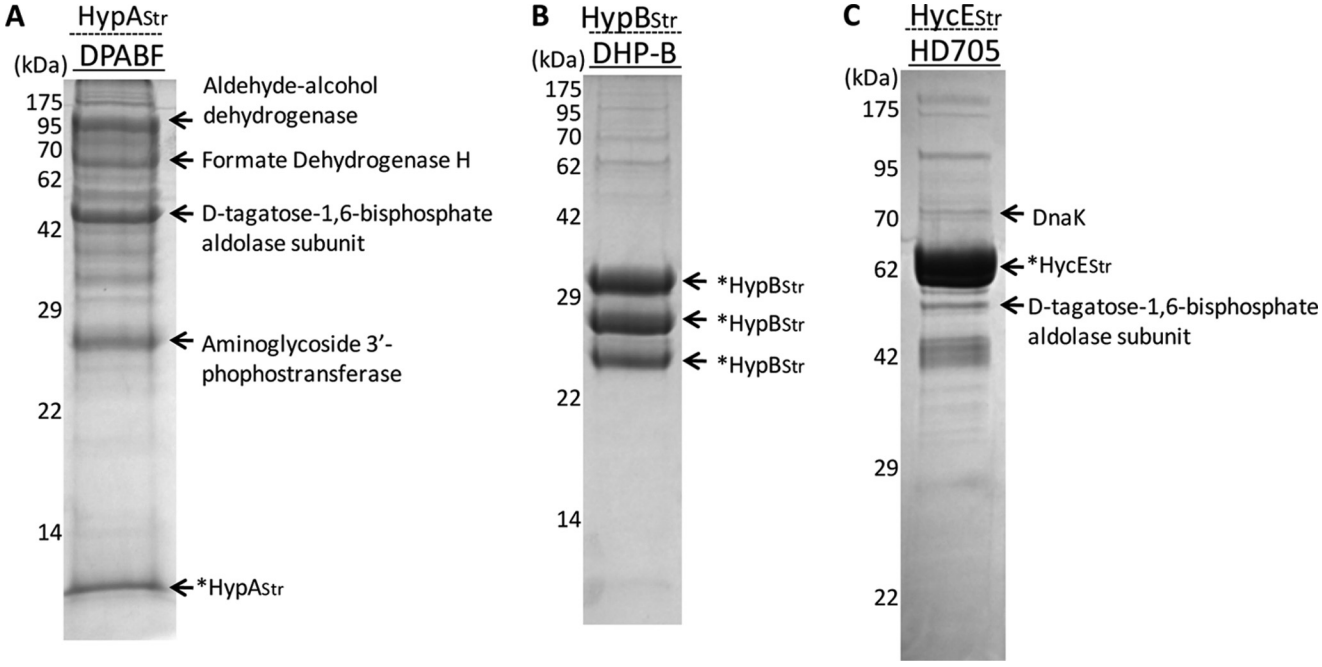

FIGURE 6. **Co-eluting proteins with HypAStr, HypBStr, or HycEStr.** The elution fractions from *Strep*-tactin-Sepharose pulldown assays from lysates of DPABF-producing HypAStr (*A*), DHP-B-producing HypBStr (*B*), and HD705-producing HycEStr (*C*) from non-cross-linked cells were resolved on 12.5% (*A* and *B*) and 10% SDS-polyacrylamide gels followed by staining with Coomassie Blue dye (*C*). Selected protein bands were cut from the gels and extracted by digestion with trypsin followed by LC-MS/MS for identification. Proteins identified by LC-MS/MS (supplemental Table S1) are labeled, and the *asterisk* indicates the bait protein used for each experiment.

HycE. Using an Alexa Fluor® 633 streptavidin conjugate to bind to HypAStr or HycEStr as well as a BODIPY® lipid probe to stain the cell membrane, cells were visualized with confocal fluorescence microscopy. Although low resolution, the HycE staining in HD705 appears to overlap with that of the lipid probe, suggesting that HycEStr localizes primarily near the membrane (Fig. 7, *A* and supplemental Fig. S8*A*). HycEStr produced in HD705 represents a mixture of HycE proteins at different stages of maturation, including the fully mature hydrogenase expected to associate with membrane-bound formate hydrogen lyase proteins. Therefore, the HYD723 strain expressing HycEStr was also stained and visualized to highlight only the nickel-free enzyme precursor, which would not be expected to assemble with the formate hydrogen lyase complex (35). However, HycEStr staining still overlapped with the BODIPY® probe (Fig. 7*B* and supplemental Fig. S8*B*), indicating that the hydrogenase precursor enzyme is found predominantly in the vicinity of the membrane region of the cell while awaiting nickel. This localization was affirmed by comparison of the fluorescence intensity profiles of the Alexa Fluor® 633

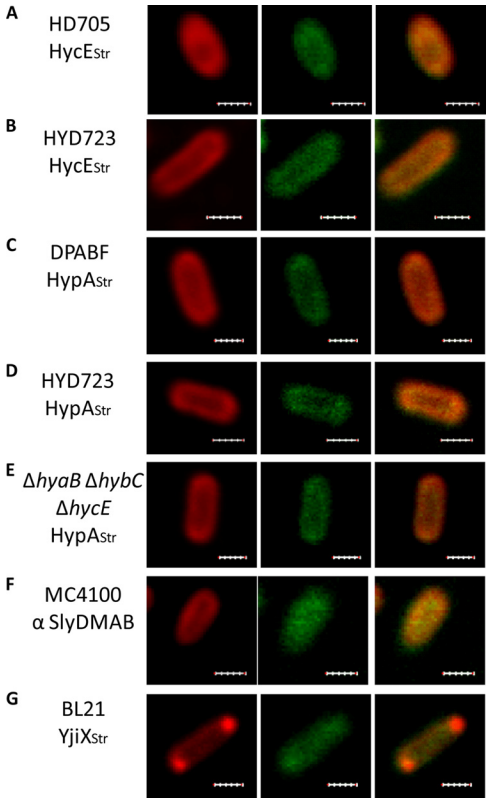

FIGURE 7. **HycEStr and HypAStr are localized near the cell membrane.** Shown are confocal fluorescence microscopy images of HD705 (*A*) and HYD723 (*B*) producing HycEStr, DPABF (*C*), HYD723 (*D*), and Δ*hyaB* Δ*hybC* Δ*hycE* (*E*) producing HypAStr, SlyD from MC4100 cells (*F*), and BL21(DE3) (*G*) producing YjiXStr. Cells were stained with BODIPY® lipid probe 558/568 (*left panels*, *red*) to visualize cell membranes and either Alexa Fluor® 633 streptavidin conjugate to visualize *Strep*-tag II HycE, HypA, and YjiX proteins or Alexa Fluor® goat anti-mouse secondary antibody to probe SlyD monoclonal antibodies (*middle panels*, *green*). The overlay of both fluorescent images is shown on the *right*. See also supplemental Fig. S8 for fluorescence profiles. *Bars* indicate 1 μm.

streptavidin to the BODIPY® lipid probe, which has similar distributions (supplemental Fig. S8*B*).

As a control, a *Strep*-tag II protein with unknown function, YjiX, was used to verify that the tag did not cause protein translocation to the membrane. Based on the sequence of YjiX, it is predicted to be a cytoplasmically localized protein by CELLO v.2.5. (subCELlular LOcalization predictor) (36). Fluorescence imaging of cells expressing YjiXStr confirmed cytoplasmic localization of the protein (Fig. 7*G* and supplemental Fig. S8*G*). In addition, monoclonal anti-SlyD antibodies were used to probe SlyD localization within the cell, and SlyD also appears to distribute throughout the cell (Fig. 7*F* and supplemental Fig. S8*F*). Given the molecular chaperone and peptidyl-prolyl isomerase activities of SlyD (37), it is not altogether surprising that this protein would be found in the cytoplasm. On the other hand, the HypAStr protein in DPABF cells exhibited similar cellular localization as HycEStr (Fig. 7*C* and supplemental Fig. S8*C*), suggesting that it also localizes proximal to the cell membrane, in agreement with the HypAStr pulldown assays of membrane proteins. HypAStr was also found near the membrane in HYD723, representing its localization before nickel acquisition (Fig. 7*D* and supplemental Fig. S8*D*). To investigate the possible differential localization of HypA before association with hydrogenase, HypAStr in the Δ*hyaB* Δ*hybC* Δ*hycE* strain was probed and detected primarily near the membrane as well (Fig. 7*E* and supplemental Fig. S8*E*), suggesting that the entire process, from nickel acquisition to nickel delivery to HycE, occurs close to the cell membrane.

DISCUSSION

It is clear that multiple accessory proteins participate in the biosynthesis of the bimetallic cluster of the [NiFe] hydrogenase enzymes (6, 9), and several of these proteins have been assigned a role in the nickel delivery stage of this process. Each of the isolated proteins can bind nickel along with other biochemical activities, but it was not clear if they interact with the hydrogenase enzyme in a coordinated manner or independent of each other. This report provides evidence consistent with a multiprotein complex containing all of the factors implicated in nickel insertion as well as the hydrogenase precursor protein itself, suggesting that these proteins cooperate together to complete this stage of hydrogenase biosynthesis.

The interactions between HypA and both HypB and SlyD in the absence of the hydrogenase 1, 2, and 3 large subunits indicates that this nickel insertion complex can preassemble before docking on the hydrogenase precursor. *In vitro* studies of purified *E. coli* and *Helicobacter pylori* proteins demonstrated that HypA and HypB can form a heterodimer (17, 18). Similarly, SlyD is pulled down with tagged HypB expressed in *E. coli* (13, 19), an association that is also observed with the purified proteins (16). These individual complexes suggest that the three proteins assemble in a quasi linear arrangement with HypB at the center, although a direct interaction between HypA and SlyD in the context of the multiprotein complex cannot be ruled out. Furthermore, some of these proteins can form homodimers in solution (11, 16, 17), so the oligomeric states in the multiprotein complexes are uncertain, although it is unlikely that dimerization by HypB is required for activity (38). The use of cross-linkers in this study does reveal multiple complexes containing each protein, which might indicate the presence of different oligomeric forms and/or association with additional proteins. Preassembly and cooperation of accessory proteins during biosynthesis of an enzyme metallocenter is a strategy employed by other systems, such as the factors involved in iron complex delivery to both [FeFe] and [NiFe] hydrogenases (39–41) and also nickel delivery to urease in *H. pylori* (7, 42). It is unclear whether preassembly of HypA, HypB, and SlyD before docking with the hydrogenase large subunit is required for nickel delivery because HypA can bind to HycE in the absence of HypB or SlyD. Furthermore, unlike HypA and HypB, SlyD can associate with the hydrogenase precursor protein before iron insertion (19). However, given the observed HypA-HypB-SlyD ternary complex, it is very possible that more than one molecule of SlyD is involved in hydrogenase maturation.

Previous experiments with tagged HycE revealed that it associates with all three nickel insertion proteins (19), but it was not established if these interactions with the hydrogenase precursor protein were dependent on each other. In this study the same proteins are observed upon pulldown of tagged HypA, suggesting that the three factors can interact concurrently in a

complex with HycE. This interpretation is based on the assumption that each protein does not form multiple pairwise interactions with all of the other components. Consistent with this model, the participation of HypB in the HycE complex depends on HypA, suggesting that HypA is the docking protein for this nickel insertion complex, as previously proposed (14). The crystal structure of HypA from *Thermococcus kodakaraensis* and the NMR structure of *H. pylori* HypA both reveal two distinct domains, one containing the zinc bound to four cysteine residues and the other containing the putative nickel ligands (21, 22). An alignment of HypA homologs indicated that the variable regions predominantly map to the zinc binding domain, suggesting that this motif is responsible for docking to the diverse sequences of the hydrogenase large subunits. Furthermore, although this domain has an unusual fold around the tetrathiolate zinc site (21, 22), it was classified into the zinc-ribbon superfamily (21), and this type of coordination is reminiscent of structural zinc ion components of domains that mediate biomolecular interactions (23). Thus it is feasible that this domain contains the interface for HycE, although this hypothesis remains to be proven. Whether or not this model can be applied for all organisms is not yet clear because other non-conserved proteins may be involved (6) and HypA was not detected in a complex of a hydrogenase large subunit from *Ralstonia eutropha* that did contain HypC and HypB (43).

The separation of hydrogenase maturation into two distinct events is supported by the isolation of incompletely mature hydrogenase proteins containing iron but not nickel (43, 44). HypCDEF proteins are responsible for the biosynthesis of the cyanide and possibly carbon monoxide ligands as well as iron insertion (6). Multiprotein complexes containing combinations of these iron accessory factors as well as the large subunit have been observed (39, 45–47). SlyD also interacts with HycE early on in maturation, suggesting that it contributes a chaperone activity in addition to its role in nickel delivery (19). The HypA, HypB, and SlyD proteins are thought to be important for nickel insertion. The finding that neither HypA nor HypB is detected in a complex with HycE in a Δ*hypC* or Δ*hypD* strain provides evidence that the activity of these proteins is dependent on completion of iron insertion, supporting two discrete stages of metal cluster assembly. It also explains the previously reported observation that nickel insertion to HycE cannot occur in DHP-C cells (48). Furthermore, these results suggest that iron insertion produces a signal such as a change in the conformation of HycE itself or in its complexes with partner proteins such as HypC that activates association with HypA and nickel delivery.

The decrease in detectable HypA-HycE complex in the Δ*nikA* strain suggests that the Nik transporter modulates this interaction and the function of HypA in hydrogenase maturation. One possible explanation is that HypA only associates with HycE upon binding nickel supplied by the Nik system. However, the H2A mutation in HypA, which abrogates hydrogenase maturation and prevents nickel binding in homologous proteins (14, 18), does not affect the interaction between HypA and the large subunit. Furthermore, even if sufficient nickel is provided through an alternative uptake pathway to produce wild-type levels of hydrogenase activity, the amount of HypA interacting with HycE is not restored to the same degree. These observations support the model that the nickel insertion accessory proteins can be bypassed by excess nickel and that their role is not to catalyze any chemical transformation but to mediate nickel delivery under nickel-limiting conditions. Moreover, the experiments reported here imply that nickel uptake through an intact Nik transporter is required for HypA activity, suggesting that there is a direct connection between the Nik transporter and the hydrogenase maturation pathway. Previous genetic studies revealed a link between *nik* regulation and hydrogenase activity (28, 49, 50) and suggested that hydrogenase maturation is supplied by a segregated pool of nickel coming through the Nik transporter. These results support a model in which, under high demand for nickel when the activity of the NikABCDE transporter is critical, nickel brought into the cell through the Nik transporter is funneled to the hydrogenase maturation pathway via the nickel insertion proteins. This model is appealing given that hydrogenase activation appears to be the sole purpose of this nickel, and a physical means to divert the metal ions to the appropriate destination would avoid competition with the many chelating biomolecules in the cytoplasm.

Further support for this model is provided by the observation that HypA is concentrated near the membrane even in the absence of the hydrogenase large subunits. Strategic localization of the nickel insertion proteins could result in proximity to the nickel transporter and a means of sequestering the incoming nickel from the rest of the cell. Whether one or more of these proteins, such as HypA, physically interact with the Nik transporter is not yet clear. No evidence for protein-protein interactions between HypAStr (this work) or HypBStr (19) and components of the Nik transporter was detected by LC-MS/MS, although this negative result may be due to the lack of detergents used in pulldown assays or the ineffectiveness of the particular cross-linker.

How HypA is directed toward the membrane is not clear. None of the primary sequences of the accessory proteins have any known membrane-localization tags. SlyD plays a role in protein translocation of partially assembled hydrogenase enyzmes through the cytoplasmic membrane as a chaperone for the twin-arginine translocation (Tat) signal sequence (51) found on some of the hydrogenase small subunits (52, 53). Upon escorting a small subunit to the membrane, SlyD could act as a focal point for the other components of the nickel insertion complex and the hydrogenase large subunit. This simplistic hypothesis is not supported, however, by the observation that SlyD appears to be broadly distributed throughout the cell. Another possible explanation is that the mRNA of one or more of the components is targeted to the membrane, as recently observed for several membrane protein-coding sequences in *E. coli* (54). However, it is not yet clear what features of the cis-acting sequences in the mRNA are required for localization.

Finally, although it has been established that the metal binding activities of all three nickel insertion proteins are required for optimal hydrogenase production, it is not known why. It is possible that these metal-binding sites each represent transfer points along the route of nickel, but some could also be allosteric metal-binding sites that activate the appropriate protein

conformations enabling nickel transfer. Further work is required to determine whether HypA not only interacts with the hydrogenase large subunit but also serves as the ultimate source of nickel.

Acknowledgments—We thank N. Khanam for the pBAD18-HypA, pBAD18-HypAStr, and pET24-YjiXStr vectors, Prof A. R. Wheeler for use of the LC-MS/MS instrument, and Dr. H. Yang and F. Xu for technical assistance. We also thank Prof. A. Böck for the generous donation of the MC4100 strains, Prof. T. K. Wood for the donation of the ΔhyaB ΔhybC ΔhycE BW25113 strain, Prof. A. Emili for the donation of the W3110 strains, Prof. M. Wahlgren for donation of the monoclonal anti-SlyD antibodies, H. Kaluarachchi, Dr. T. Ngu, and A. Sydor for critical reading of this manuscript, and members of the Zamble laboratory for helpful discussions.

REFERENCES

1. Forzi, L., and Sawers, R. G. (2007) *Biometals* **20,** 565–578
2. Ballantine, S. P., and Boxer, D. H. (1985) *J. Bacteriol.* **163,** 454–459
3. Redwood, M. D., Mikheenko, I. P., Sargent, F., and Macaskie, L. E. (2008) *FEMS Microbiol. Lett.* **278,** 48–55
4. McGlynn, S. E., Mulder, D. W., Shepard, E. M., Broderick, J. B., and Peters, J. W. (2009) *Dalton Trans* **22,** 4274–4285
5. Fontecilla-Camps, J. C., Volbeda, A., Cavazza, C., and Nicolet, Y. (2007) *Chem. Rev.* **107,** 4273–4303
6. Böck, A., King, P. W., Blokesch, M., and Posewitz, M. C. (2006) *Adv. Microb. Physiol.* **51,** 1–71
7. Kuchar, J., and Hausinger, R. P. (2004) *Chem. Rev.* **104,** 509–525
8. Li, Y., and Zamble, D. B. (2009) *Chem. Rev.* **109,** 4617–4643
9. Kaluarachchi, H., Chan Chung, K. C., and Zamble, D. B. (2010) *Nat. Prod. Rep.* **27,** 681–694
10. Rossmann, R., Sauter, M., Lottspeich, F., and Böck, A. (1994) *Eur. J. Biochem.* **220,** 377–384
11. Maier, T., Jacobi, A., Sauter, M., and Böck, A. (1993) *J. Bacteriol.* **175,** 630–635
12. Hube, M., Blokesch, M., and Böck, A. (2002) *J. Bacteriol.* **184,** 3879–3885
13. Zhang, J. W., Butland, G., Greenblatt, J. F., Emili, A., and Zamble, D. B. (2005) *J. Biol. Chem.* **280,** 4360–4366
14. Blokesch, M., Rohrmoser, M., Rode, S., and Böck, A. (2004) *J. Bacteriol.* **186,** 2603–2611
15. Dias, A. V., Mulvihill, C. M., Leach, M. R., Pickering, I. J., George, G. N., and Zamble, D. B. (2008) *Biochemistry* **47,** 11981–11991
16. Leach, M. R., Zhang, J. W., and Zamble, D. B. (2007) *J. Biol. Chem.* **282,** 16177–16186
17. Atanassova, A., and Zamble, D. B. (2005) *J. Bacteriol.* **187,** 4689–4697
18. Mehta, N., Olson, J. W., and Maier, R. J. (2003) *J. Bacteriol.* **185,** 726–734
19. Chan Chung, K. C., and Zamble, D. B. (2011) *FEBS Lett.* **585,** 291–294
20. Herbst, R. W., Perovic, I., Martin-Diaconescu, V., O'Brien, K., Chivers, P. T., Pochapsky, S. S., Pochapsky, T. C., and Maroney, M. J. (2010) *J. Am. Chem. Soc.* **132,** 10338–10351
21. Watanabe, S., Arai, T., Matsumi, R., Atomi, H., Imanaka, T., and Miki, K. (2009) *J. Mol. Biol.* **394,** 448–459
22. Xia, W., Li, H., Sze, K. H., and Sun, H. (2009) *J. Am. Chem. Soc.* **131,** 10031–10040
23. Gamsjaeger, R., Liew, C. K., Loughlin, F. E., Crossley, M., and Mackay, J. P. (2007) *Trends Biochem. Sci.* **32,** 63–70
24. Guzman, L. M., Belin, D., Carson, M. J., and Beckwith, J. (1995) *J. Bacteriol.* **177,** 4121–4130
25. Blokesch, M., Paschos, A., Theodoratou, E., Bauer, A., Hube, M., Huth, S., and Böck, A. (2002) *Biochem. Soc. Trans.* **30,** 674–680
26. Wu, L. F., and Mandrand-Berthelot, M. A. (1986) *Biochimie* **68,** 167–179
27. Theodoratou, E., Huber, R., and Böck, A. (2005) *Biochem. Soc. Trans.* **33,** 108–111
28. Wu, L. F., Mandrand-Berthelot, M. A., Waugh, R., Edmonds, C. J., Holt, S. E., and Boxer, D. H. (1989) *Mol. Microbiol.* **3,** 1709–1718
29. Sawers, R. G. (2005) *Biochem. Soc. Trans.* **33,** 42–46
30. UniProt Consortium (2011) *Nucleic Acids Res.* **39,** D214–D219
31. Kessler, D., Leibrecht, I., and Knappe, J. (1991) *FEBS Lett.* **281,** 59–63
32. Eppler, T., Postma, P., Schütz, A., Völker, U., and Boos, W. (2002) *J. Bacteriol.* **184,** 3044–3052
33. Nobelmann, B., and Lengeler, J. W. (1996) *J. Bacteriol.* **178,** 6790–6795
34. Varga, M. E., and Weiner, J. H. (1995) *Biochem. Cell Biol.* **73,** 147–153
35. Magalon, A., and Böck, A. (2000) *FEBS Lett.* **473,** 254–258
36. Yu, C. S., Lin, C. J., and Hwang, J. K. (2004) *Protein Sci.* **13,** 1402–1406
37. Scholz, C., Eckert, B., Hagn, F., Schaarschmidt, P., Balbach, J., and Schmid, F. X. (2006) *Biochemistry* **45,** 20–33
38. Cai, F., Ngu, T. T., Kaluarachchi, H., and Zamble, D. B. (2011) *J. Biol. Inorg. Chem.* **16,** 857–868
39. Jones, A. K., Lenz, O., Strack, A., Buhrke, T., and Friedrich, B. (2004) *Biochemistry* **43,** 13467–13477
40. Mansure, J. J., and Hallenbeck, P. C. (2008) *Biotechnol. Lett.* **30,** 1765–1769
41. McGlynn, S. E., Ruebush, S. S., Naumov, A., Nagy, L. E., Dubini, A., King, P. W., Broderick, J. B., Posewitz, M. C., and Peters, J. W. (2007) *J. Biol. Inorg. Chem.* **12,** 443–447
42. Stingl, K., Schauer, K., Ecobichon, C., Labigne, A., Lenormand, P., Rousselle, J. C., Namane, A., and de Reuse, H. (2008) *Mol. Cell. Proteomics* **7,** 2429–2441
43. Winter, G., Buhrke, T., Lenz, O., Jones, A. K., Forgber, M., and Friedrich, B. (2005) *FEBS Lett.* **579,** 4292–4296
44. Löscher, S., Zebger, I., Andersen, L. K., Hildebrandt, P., Meyer-Klaucke, W., and Haumann, M. (2005) *FEBS Lett.* **579,** 4287–4291
45. Blokesch, M., and Böck, A. (2002) *J. Mol. Biol.* **324,** 287–296
46. Butland, G., Zhang, J. W., Yang, W., Sheung, A., Wong, P., Greenblatt, J. F., Emili, A., and Zamble, D. B. (2006) *FEBS Lett.* **580,** 677–681
47. Blokesch, M., Paschos, A., Bauer, A., Reissmann, S., Drapal, N., and Böck, A. (2004) *Eur. J. Biochem.* **271,** 3428–3436
48. Magalon, A., and Bock, A. (2000) *J. Biol. Chem.* **275,** 21114–21120
49. Rowe, J. L., Starnes, G. L., and Chivers, P. T. (2005) *J. Bacteriol.* **187,** 6317–6323
50. Iwig, J. S., Rowe, J. L., and Chivers, P. T. (2006) *Mol. Microbiol.* **62,** 252–262
51. Graubner, W., Schierhorn, A., and Brüser, T. (2007) *J. Biol. Chem.* **282,** 7116–7124
52. Wu, L. F., Chanal, A., and Rodrigue, A. (2000) *Arch. Microbiol.* **173,** 319–324
53. Dubini, A., and Sargent, F. (2003) *FEBS Lett.* **549,** 141–146
54. Nevo-Dinur, K., Nussbaum-Shochat, A., Ben-Yehuda, S., and Amster-Choder, O. (2011) *Science* **331,** 1081–1084
55. Casadaban, M. J., and Cohen, S. N. (1979) *Proc. Natl. Acad. Sci. U.S.A.* **76,** 4530–4533
56. Sauter, M., Böhm, R., and Böck, A. (1992) *Mol. Microbiol.* **6,** 1523–1532
57. Jacobi, A., Rossmann, R., and Böck, A. (1992) *Arch. Microbiol.* **158,** 444–451
58. Maeda, T., Sanchez-Torres, V., and Wood, T. K. (2007) *Appl. Microbiol. Biotechnol.* **77,** 879–890